A novel, noncatalytic carbohydrate-binding module displays specificity for galactose-containing polysaccharides through calcium-mediated oligomerization

Cédric Montanier, Márcia a S Correia, James E Flint, Yanping Zhu, Arnaud Baslé, Lauren S Mckee, José a M Prates, Samuel J Polizzi, Pedro M Coutinho, Richard J Lewis, et al.

HAL Id: hal-02652804
https://hal.inrae.fr/hal-02652804v1

Submitted on 29 May 2020

A Novel, Noncatalytic Carbohydrate-binding Module Displays Specificity for Galactose-containing Polysaccharides through Calcium-mediated Oligomerization*[S]

Cedric Y. Montanier[‡1], Márcia A. S. Correia[§1], James E. Flint[‡1], Yanping Zhu[‡§¶1], Arnaud Baslé[‡], Lauren S. McKee[‡¶], José A. M. Prates[§], Samuel J. Polizzi[‖], Pedro M. Coutinho**, Richard J. Lewis[‡], Bernard Henrissat**, Carlos M. G. A. Fontes[§2], and Harry J. Gilbert[‡¶3]

From the §Centro de Investigação Interdisciplinar em Sanidade Animal, Faculdade de Medicina Veterinária, Universidade Técnica de Lisboa, Avenida da Universidade Técnica, 1300-477 Lisboa, Portugal, the ‡Institute for Cell and Molecular Biosciences, Newcastle University, Medical School, Newcastle upon Tyne NE2 4HH, United Kingdom, the **Architecture et Fonction des Macromolécules Biologiques, UMR6098, CNRS, Universités Aix-Marseille I and II, 163 Avenue de Luminy, 13288 Marseille, France, the ¶Complex Carbohydrate Research Center, University of Georgia, Athens, Georgia 30602-4712, and the ‖Department of Biochemistry and Molecular Biology, University of Georgia, Athens, Georgia 30602-7229

The enzymic degradation of plant cell walls plays a central role in the carbon cycle and is of increasing environmental and industrial significance. The catalytic modules of enzymes that catalyze this process are generally appended to noncatalytic carbohydrate-binding modules (CBMs). CBMs potentiate the rate of catalysis by bringing their cognate enzymes into intimate contact with the target substrate. A powerful plant cell wall-degrading system is the *Clostridium thermocellum* multienzyme complex, termed the "cellulosome." Here, we identify a novel CBM (*Ct*CBM62) within the large *C. thermocellum* cellulosomal protein Cthe_2193 (defined as *Ct*Xyl5A), which establishes a new CBM family. Phylogenetic analysis of CBM62 members indicates that a circular permutation occurred within the family. *Ct*CBM62 binds to D-galactose and L-arabinopyranose in either anomeric configuration. The crystal structures of *Ct*CBM62, in complex with oligosaccharides containing α- and β-galactose residues, show that the ligand-binding site in the β-sandwich protein is located in the loops that connect the two β-sheets. Specificity is conferred through numerous interactions with the axial O4 of the target sugars, a feature that distinguishes galactose and arabinose from the other major sugars located in plant cell walls. *Ct*CBM62 displays tighter affinity for multivalent ligands compared with molecules containing single galactose residues, which is associated with precipitation of these complex carbohydrates. These avidity effects, which confer the targeting of polysaccharides, are mediated by calcium-dependent oligomerization of the CBM.

Carbohydrate protein recognition plays a central role in biology, exemplified by microbe-mediated plant cell wall degradation. The release of sugars from plant cell walls is not only critical for the maintenance of the carbon cycle but is of increasing industrial and environmental significance through the development of second generation lignocellulose-based biofuels (1). The chemical and physical complexity of plant cell walls restricts their accessibility to enzyme attack and thus the recycling of photosynthetically fixed carbon is a relatively slow biological process.

Enzymes that catalyze plant cell wall degradation display complex molecular architectures. In addition to the catalytic module(s), these enzymes often contain one or more noncatalytic carbohydrate-binding modules (CBMs)[4] (2). CBMs, by binding to their target ligand, bring the appended enzymes into intimate contact with its substrate thereby potentiating catalysis by reducing the accessibility problem (3–5). Carbohydrate-modifying enzymes and their component modules, which include CBMs, have been classified into sequence-based families in the CAZy database (6). Currently, there are 61 families of CBMs that recognize a variety of plant and mammalian glycans. In some families, exemplified by CBM1 and CBM10, ligand specificity is invariant; however, it is becoming increasingly apparent that carbohydrate recognition can be highly variable in different members of the same family. For example, CBM6 contains members that recognize xylan (β-1,4-xylose polymer), single cellulose (β-1,4-glucose polymer) chains, mixed linked β-1,4-β-1,3-glucans, laminarin (β-1,3-glucose polymer), and agarobiose (3,6-anhydro-L-galactose-D-galactose) (7–10).

Representative three-dimensional structures of around half the CBM families are available. The majority of these proteins display a β-sandwich fold in which the ligand-binding site for

[S] The on-line version of this article (available at http://www.jbc.org) contains supplemental Figs. S1 and S2 and Tables S1 and S2.
The atomic coordinates and structure factors (codes 2YFU, 2YFZ, and 2YG0) have been deposited in the Protein Data Bank, Research Collaboratory for Structural Bioinformatics, Rutgers University, New Brunswick, NJ (http://www.rcsb.org/).
The nucleotide sequence(s) reported in this paper has been submitted to the GenBank™/EBI Data Bank with accession number(s) ABN53395.1.
[1] These authors contributed equally to this work.
[2] To whom correspondence may be addressed. E-mail: cafontes@fmv.utl.pt.
[3] To whom correspondence may be addressed: Institute for Cell and Molecular Biosciences, Newcastle University, Medical School, Framlington Place, Newcastle upon Tyne NE2 4HH, United Kingdom. E-mail: h.j.gilbert@newcastle.ac.uk.

[4] The abbreviations used are: CBM, carbohydrate-binding module; PDB, Protein Data Bank; r.m.s.d., root mean square deviation; ITC, isothermal titration calorimetry.

extended glycan chains is generally located on the β-sheet that includes the concave surface of the protein (for review see Ref. 2). For CBMs that recognize terminal mono- or disaccharides, the ligand-binding site is often located in the loops that connect the two β-sheets. Although there are examples of CBMs where the orientation of aromatic residues confers ligand specificity (12, 13), it is increasingly evident that polar interactions play a more important role in carbohydrate recognition (8, 9, 14). Recent reports have also revealed examples of CBMs that harness calcium in ligand recognition (8, 15, 16). CBMs are generally located in monomeric enzymes; thus cooperative (or avidity) effects occur rarely. Exceptions to this general rule are evident, however, in enzymes that contain multiple copies of CBMs that display the same specificity, where avidity effects between these modules has led to increased affinity for polysaccharides such as xylan (17–19). Given that oligomerization is a general feature of lectins (carbohydrate binding domains that are not components of enzymes), where avidity effects are common (20), it is surprising that similar macromolecular associations have not been observed in the CBM literature.

The multienzyme complex expressed by *Clostridium thermocellum,* referred to as the "cellulosome," is one of the most powerful and intricate plant cell wall-degrading systems described to date (21, 22). The enzyme complex is anchored onto the plant cell wall by the noncatalytic scaffoldin protein, which contains a family 3 CBM that binds to crystalline cellulose (23). The catalytic subunits of the cellulosome also contain CBMs, which target β-glucans, xylans, uronic acids, and chitin (7, 16, 24–27), which direct the complex toward the target substrates for these enzymes. The extent to which the cellulosome can be directed toward the myriad of carbohydrate structures in plant cell wall, however, remains relatively unexplored, and indeed, numerous cellulosomal proteins contain modules of unknown function that could, potentially, comprise CBMs that display novel specificities. Furthermore, the quaternary structure of the cellulosome may provide a background for cooperativity between the CBMs within this protein complex, although such interactions have not been observed experimentally.

Here, we report the structure and biochemistry of a module, defined as *Ct*CBM62, of the *C. thermocellum* cellulosomal protein Cthe_2193 (GenBank[TM] protein accession ABN53395.1; defined hereafter as *Ct*Xyl5A) that exhibits no significant sequence similarity to CBMs in the CAZy database. *Ct*CBM62 displays a β-sandwich fold that binds to terminal α- and β-D-galactopyranose or L-arabinopyranose residues of complex polysaccharides. Ligand specificity is conferred primarily through extensive interactions with the axial O4 of galactose and arabinose, a distinctive feature of these two sugars. *Ct*CBM62 also displays calcium-mediated oligomerization resulting in avidity effects that confer selectivity for polysaccharides rather than monovalent oligosaccharides.

EXPERIMENTAL PROCEDURES

Cloning, Expression, and Purification of Components of Cthe_2193—DNA encoding the following regions of *Ct*Xyl5A, GH5-CBM6-CBM13-Fn3-*Ct*CBM62 Docl (mature *Ct*Xyl5A; see Fig. 1) and *Ct*CBM62, were amplified using primers, containing

NheI and XhoI restriction sites, listed in supplemental Table S1. The amplified DNAs were cloned into NheI/XhoI-restricted pET21a, such that the encoded recombinant proteins contain a C-terminal His$_6$ tag. To express the two *C. thermocellum* proteins, *Escherichia coli* strain BL21(DE3), harboring appropriate recombinant plasmids, was cultured to mid-exponential phase in Luria broth at 37 °C followed by the addition of isopropyl β-D-galactopyranoside at 1 mM, to induce recombinant gene expression, and incubated for a further 5 h at 37 °C. The recombinant proteins were purified to >90% electrophoretic purity by immobilized metal ion affinity chromatography using Talon[TM], a cobalt-based matrix, and eluted with 100 mM imidazole, as described previously (19). When preparing the selenomethionine derivative of *Ct*CBM62 for crystallography, the protein was expressed in *E. coli* B834 (DE3), a methionine auxotroph, cultured in media comprising 1 liter of SelenoMet Medium Base[TM], 50 ml of SelenoMet Nutrient Mix[TM], and 4 ml of selenomethionine solution (10 mg/ml). Recombinant gene expression was as described above, as was protein purification, except that all buffers were supplemented with 10 mM β-mercaptoethanol.

Mutagenesis—Site-directed mutagenesis was carried out using the PCR-based QuikChange method (Stratagene) deploying the primers listed in supplemental Table S1.

Binding Assays—Affinity gel electrophoresis was used to screen for the binding of *Ct*CBM62 to polysaccharides, following the method of Ref. 28. The proteins were subjected to nondenaturing PAGE, in the presence of 5 mM CaCl$_2$, deploying parallel gels containing no ligand and the target polysaccharide at 100 μg/ml, respectively. The gels were also loaded with BSA, which acts as a nonbinding negative control. After electrophoresis, the gels were stained with Coomassie Blue, and proteins that bound to the polysaccharide displayed reduced electrophoretic migration in the presence of the complex carbohydrate. The binding of *Ct*CBM62 to its ligands was quantified by isothermal titration calorimetry (ITC), as described previously (25). Titrations were carried out in 50 mM Na-HEPES buffer, pH 7.5, containing 5 mM CaCl$_2$ (or 5 mM EDTA) at 25 °C. The reaction cell contained protein at 145 μM, while the syringe contained either the oligosaccharide at 10 mM or polysaccharide at 3–5 mg/ml. The titrations were analyzed using Microcal Origin version 7.0 software to derive n, K_a, and ΔH values, although ΔS was calculated using the standard thermodynamic equation, $RT\ln K_a = \Delta G = \Delta H - T\Delta S$.

Analytical Ultracentrifugation—Sedimentation velocity experiments were performed using an Optima XLA analytical ultracentrifuge (Beckman Coulter) with an An60 Ti four-hole rotor. Purified *Ct*CBM62 (see above) was dialyzed into either CaCl$_2$ buffer (50 mM Na-HEPES, pH 7.5, 150 mM NaCl, 10 mM CaCl$_2$) or EDTA buffer (50 mM Na-HEPES, pH 7.5, 150 mM NaCl, 10 mM EDTA) using a Microdialyzer System 100 (Pierce). In each experiment, 400 μl of 1 mg/ml *Ct*CBM62 and 410 μl of reference buffer were loaded into 12-mm double-sector Epon centerpieces equipped with quartz windows and equilibrated for ~1 h at 20 °C. Experiments were performed at a rotor speed of 50,000 rpm and a wavelength of 280 nm. Data were collected over 8.5-h periods using a radial step size of 0.003 cm. The partial specific volume ($\bar{v}$) of 0.7211 was calculated from the

TABLE 1

Diffraction data collection and refinement statistics of *Ct*CBM62

Values in parentheses refer to the highest resolution shell.

	*Ct*CBM62 SeMet	*Ct*CBM62 native	*Ct*CBM62/xyloglucan oligosaccharide	*Ct*CBM62/GM3
Data collection				
Wavelength	1.54	1.54	1.073	1.073
Space group cell dimensions	F432	F432	F432	F432
a, b, c	$a = b = c = 191.75$ Å	$a = b = c = 192.16$ Å	$a = b = c = 191.82$ Å	$a = b = c = 191.72$ Å
Resolution	47.94–2.43 Å	48.04–1.65 Å	44–1.80 Å	47.93–1.80 Å
	(2.56–2.43 Å)	(1.74–1.65 Å)	(1.90–1.80 Å)	(1.90–1.80 Å)
R_{merge}	0.113 (0.453)	0.066 (0.406)	0.113 (0.537)	0.081 (0.479)
$I/\sigma I$	47.5 (12.1)	33.7 (7.1)	18.2 (4.6)	21.9 (5.4)
Completeness	99.9% (99.1%)	100.0% (99.8%)	100.0% (100.0%)	99.8% (100.0%)
Redundancy	53.7 (43.3)	15.7 (13.2)	10.5 (10.6)	10.4 (10.5)
Anomalous completeness	99.7% (98.1%)			
Anomalous redundancy	29.7 (23.2)			
Refinement				
No. of reflections	–	37038 (5272)	21020 (2996)	28437 (4098)
R_{work}/R_{free}	–	0.1512 (0.1624)	0.1637 (0.1803)	0.1621 (0.1787)
No. of atoms				
Protein	–	1058	1061	1053
Ligand/Ion	–	13	64	30
Water	–	224	136	190
B-factor				
Protein	–	13	12	15
Ligand/Ion	–	19	47	26
Water	–	28	24	29
Root mean square deviations				
Bond lengths		0.015 Å	0.014 Å	0.014 Å
Bond angles		1.42°	1.29°	1.69°
PDB codes		2YFU	2YFZ	2YG0

amino acid sequence. The buffer viscosity of 0.00892 centipoise and density of 1.0042 g/ml for the CaCl$_2$ buffer or 1.005 g/ml for the EDTA buffer were calculated using the program SEDN-TERP. All data analysis for sedimentation velocity experiments were performed using the program SEDFIT, version 12.1b. Continuous sedimentation coefficient distribution *c*(*s*) analyses were restrained by Marquardt-Levenberg regularization at a confidence interval $p = 0.68$ with uniform prior knowledge (29). The base line, meniscus, frictional coefficient, systematic time invariant, and radial invariant noise were fitted. The final fit $c^{(P\delta)}(s)$ implemented prior knowledge of discrete species for determining the size distribution (30). The r.m.s.d. values for all reported experiments were 0.008 or less.

Crystallography—*Ct*CBM62 was crystallized using the hanging drop vapor diffusion technique at 20 °C with an equal volume (1 μl) of protein and reservoir solution. The native and selenomethionine (in the presence of 5 mM DTT) forms of apo-*Ct*CBM62 were crystallized in 20% (w/v) PEG 3350, 0.2 M trisodium citrate, pH 8.3 (PEG/Ion™ 1 screen condition 46; Hampton Research) at 150 mg/ml. *Ct*CBM62 in complex with 10 mM xyloglucan oligosaccharides was crystallized in the same condition described above at a protein concentration of 191 mg/ml. *Ct*CBM62, in complex with 10 mM ^{1}6-α-GalMan$_3$, was crystallized in 0.5 M ammonium sulfate in 0.1 M Na-HEPES, pH 7.4, containing 30% 2-methyl-2,4-pentanediol (condition 59 of the PACT screen) also with protein at 191 mg/ml. The *Ct*CBM62 crystals grew over 4–5 days, after which 25 μl of mother liquor, including 30% (v/v) glycerol, was added as the cryoprotectant before being flash frozen in liquid nitrogen.

All the crystals of *Ct*CBM62 were in space group F432 with unit cell dimensions of $a = b = c = 192.2$ Å, with one protein molecule in the asymmetric unit. The structure of apo-

*Ct*CBM62 was solved by SIRAS, exploiting both the anomalous scattering from the seleniums and the isomorphous differences between the selenomethionine derivative and the native diffraction data. After processing the diffraction data in XDS (31) and SCALA (32), the unmerged intensities were input to the HKL2MAP (33) interface to SHELX (34), and the heavy atom substructure was solved in SHELXD. The SHELXE solvent flattened map was of sufficient quality to build manually, in COOT (35), the *Ct*CBM62 molecule. The ligand-bound structures of *Ct*CBM62 were determined by molecular replacement with AMORE (36) using the apo structure as the search model. All structures were refined to convergence using REFMAC5 (37) with manual corrections being applied in COOT (35). The data collection, phasing, and refinement statistics are displayed in Table 1, and the PDB codes for the protein structures are as follows: 2YFU, 2YFZ, and 2YG0.

RESULTS

CtCBM62 Is a Component of the C. thermocellum Cellulosomal Protein CtXyl5A—An initial analysis of the *C. thermocellum* genome was performed as described in Cantarel *et al.* (6). The analysis identified 72 genes encoding modular proteins with elements corresponding to CAZy families of catalytic modules and CBMs, which, based on the presence of type I dockerins, were components of the cellulosome. The functions of many of these proteins have been demonstrated biochemically or inferred from sequence similarity to enzymes with known activities. There remain, however, several cellulosomal subunits that contain modules with no sequence similarity with proteins of known function. The open reading frame identified as locus Cthe_2193 (defined hereafter as *Ct*Xyl5A) is one such protein. The protein is likely to be secreted because it contains

an N-terminal 20-residue signal peptide. The mature polypeptide includes 928 amino acids and consists of six modules, which are displayed in Fig. 1. In addition to the type I dockerin, the protein contains two CBMs from families 6 and 13, a fibronectin domain, and a GH5 module, which is likely to be the catalytic component of the protein (see the accompanying paper, which describes the biochemical properties of the full-length enzyme (38)). A particularly noteworthy feature of the open reading frame is the sequence extending from 740 to 878, defined hereafter as *Ct*CBM62, which displays no significant sequence similarity to proteins in the CAZy database. To investigate the function of *Ct*CBM62, a recombinant form of this protein module was expressed in soluble form in *E. coli* and purified to electrophoretic homogeneity.
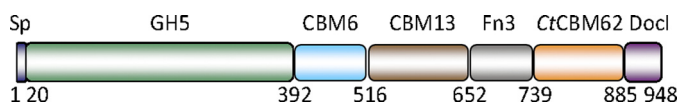

FIGURE 1. **Schematic of CtXyl5A.** The abbreviated modules are as follows: *Sp,* signal peptide; *DocI,* type I dockerin modules.

TABLE 2

Polysaccharide specificity of CtCBM62 determined by affinity polyacrylamide gel electrophoresis

Ligand[a]	Binding[b]
Arabinogalactan	++
Oat-spelt xylan	−
Wheat arabinoxylan	−
Laminarin	−
Lichenan (Icelandic moss)	−
Xyloglucan (Tamarind)	+++
Glucomannan (Konjac)	−
Galactomannan (Gal:Man, 21:79) (Carob)	++
Galactomannan (Gal:Man, 38:40) (Guar)	+++
Pullulan	−
Galactan (Potato)	−
Pustulan	−
Rhamnogalacturonan (Soybean)	−
Hydroxyethylcellulose	−
Glucuronoxylan	−
Arabinan (debranched)	−
Pectic galactan (Potato)	−
Polygalacturonic acid	−
Rhamnogalacturonan I (Potato)	−

[a] Ligands were screened at a concentration of 0.1 mg/ml.
[b] The following symbols are used: −, no detectable binding; ++, significant binding; +++, strong binding +++.

Identification of a Novel CBM in CtXyl5A—Biochemical analysis of *Ct*CBM62 failed to reveal catalytic activity against an extensive range of plant structural polysaccharides, including cellulose and various hemicellulose and pectin polymers (data not shown). To explore whether *Ct*CBM62 fulfills a noncatalytic carbohydrate binding function, the capacity of the protein to bind to a range of polysaccharides was assessed by affinity gel electrophoresis. The data, reported in Table 2, show that the protein module binds to xyloglucan, arabinogalactan, and galactomannan, but does not recognize the other polymers evaluated, including the arabinoxylans that are hydrolyzed by *Ct*Xyl5A (38). The protein module therefore includes a functional CBM and represents the founding member of a new family designated CBM62. To investigate the specificity of *Ct*CBM62 in more detail, the capacity of the protein to bind to galactomannan- and xyloglucan-derived oligosaccharides and monosaccharides was assessed by ITC. The data, reported in Table 3, with example titrations displayed in Fig. 2, show that *Ct*CBM62 does not bind to mannooligosaccharides or cellulooligosaccharides, the backbone structures of galactomannan and xyloglucan, respectively, or the repeating *XXXG* (*X* is a backbone glucose decorated $\alpha1,6$ with Xyl and G represents unsubstituted glucose) motif of xyloglucan (39). The protein, however, does bind to ^{1}6-α-D-GalMan$_3$, ^{3}6^{4}6-α-D-Gal$_2$Man$_5$, and a mixture of *XLXG*, *XLLG*, and *XXLG*, where *L* is *X* in which the xylose is decorated with a $\beta1,2$-linked D-galactose residue. The stoichiometry of binding was unity for galactose residues (in the oligosaccharides) indicating that *Ct*CBM62 has a single ligand-binding site. The thermodynamic data show that the binding of *Ct*CBM62 to all its ligands is enthalpically driven, whereas the change in entropy makes a negative contribution to overall affinity, as observed for the majority of CBMs studied to date (14, 16, 27). These data indicate that *Ct*CBM62 binds to galactomannan, arabinogalactan, and xyloglucan, which are all decorated with galactose residues, through recognition of the hexose sugar. This view was confirmed by the observation that the protein binds to galactose and arabinose, in which O4 is axial, but not to sugars such as xylose, mannose, and glucose, where O4 is equatorial. Indeed, the similar affinity of *Ct*CBM62 for ^{1}6-α-D-GalMan$_3$ and galactose, and the lack of significant

TABLE 3

Affinity and thermodynamic parameters of CtCBM62 binding to polysaccharides, oligosaccharides and monosaccharides

Ligand	$K_a \times 10^4$	ΔG	ΔH	$T\Delta S$	n^a
	$_M{}^{-1}$	$kcal\ mol^{-1}$	$kcal\ mol^{-1}$	$kcal\ mol^{-1}$	
Galactomannan (Carob)	56.4 ± 3.1	−7.85 ± 0.03	−11.23 ± 0.06	−3.38 ± 0.03	1.00 ± 0.003
$6^3,6^4$-Di-α-D-galactosyl mannopentaose	2.21 ± 0.72	−4.56 ± 1.14	−8.69 ± 1.6	−4.13 ± 0.46	0.992 ± 0.15
6^1-α-D-Galactosyl mannotriose	0.29 ± 0.02	−4.33 ± 0.03	−7.04 ± 0.75	−2.71 ± 0.72	1.07 ± 0.89
Galactose	0.32 ± 0.003	−4.79 ± 0.01	−8.59 ± 0.17	−3.8 ± 0.16	1.07 ± 0.02
Mannopentaose	NB[b]				
Xyloglucan (Tamarind)	177 ± 17.7	−8.53 ± 0.06	−11.63 ± 0.07	−3.1 ± 0.01	1.01 ± 0.003
XLXLG	2.01 ± 0.20	−5.87 ± 0.06	−10.74 ± 0.46	−4.87 ± 0.40	1.08 ± 0.036
XXXG	<0.01				
Arabinogalactan (Larch)	84.1 ± 8.4	−8.09 ± 0.06	−13.16 ± 0.10	−5.07 ± 0.04	1.04 ± 0.005
Arabinan (debranched)	9.42 ± 0.49	−6.79 ± 0.03	−10.84 ± 0.10	−4.05 ± 0.07	1.02 ± 0.007
Arabinose	0.11 ± 0.005	−4.17 ± 0.02	−9.10 ± 0.20	−4.93 ± 0.18	0.99 ± 0.22
Xylan (oat spelt)	<0.01				
Cellohexaose	NB				
Cellotetraose	NB				
Xylose	NB				

[a] The ITC data were fitted to a single site binding model for all ligands. For polysaccharide ligands, in which the molar concentration of binding sites is unknown, the *n* value was iteratively fitted as close as possible to one, by adjusting the molar concentration of the ligand.
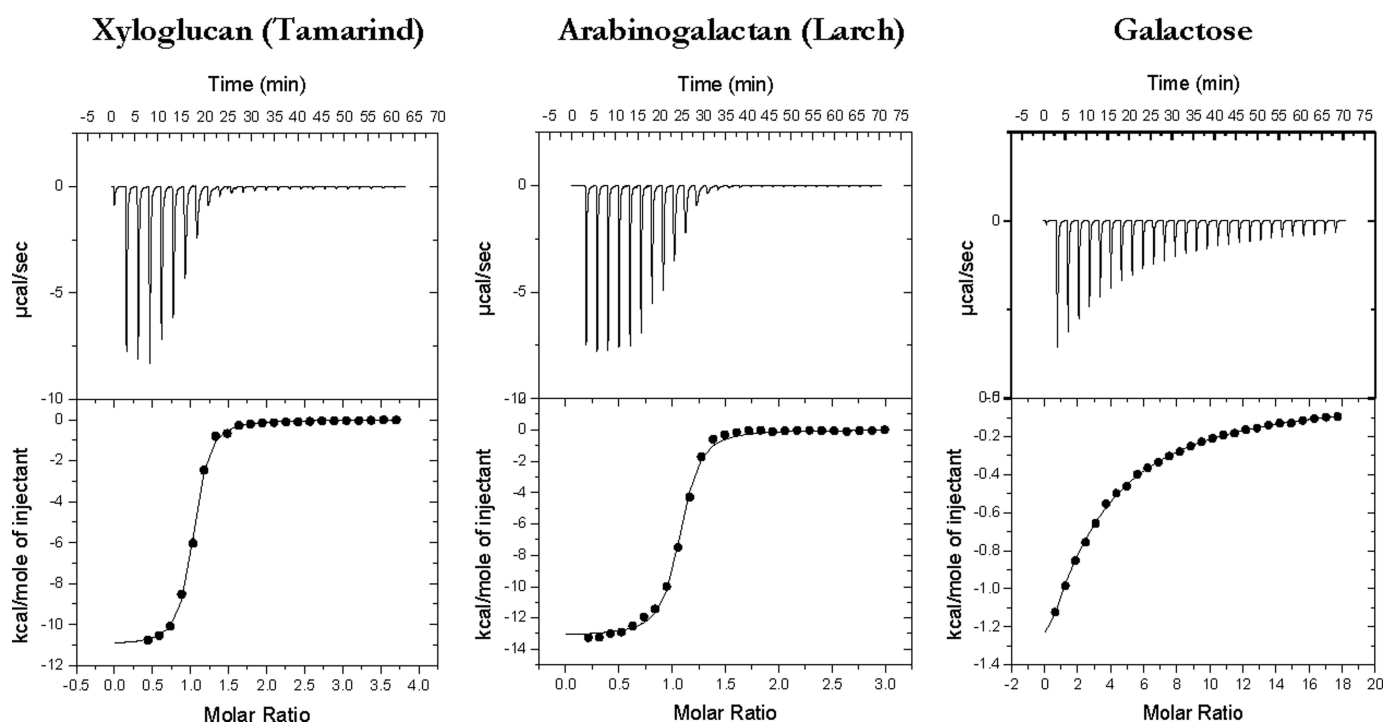[b] NB, no binding.

FIGURE 2. **Representative ITC data of *Ct*CBM62 binding to soluble ligands.** The ligand (3 mg/ml xyloglucan, 5 mg/ml arabinogalactan, 10 mM arabinose) in the syringe was titrated into *Ct*CBM52 (145 μM) in the cell. The *top half* of each panel shows the raw ITC heats; the *bottom half* shows the integrated peak areas fitted using a one single binding model by MicroCal Origin software. ITC was carried out in 50 mM Na-HEPES, pH 7.5, containing 5 mM CaCl$_2$, at 25 °C.

TABLE 4

The influence of calcium on the affinity of *Ct*CBM62 for xyloglucan and galactose

Ligand	$K_a \times 10^4$	ΔG	ΔH	$T\Delta S$	n[a]
	M^{-1}	*kcal mol*$^{-1}$	*kcal mol*$^{-1}$	*kcal mol*$^{-1}$	
Xyloglucan + calcium[b]	129 ± 14.3	-8.35 ± 0.07	-11.4 ± 0.11	-3.14 ± 0.18	1.00 ± 0.004
Xyloglucan − calcium[c]	0.95 ± 0.02	-5.43 ± 0.01	-11.5 ± 0.15	-6.08 ± 0.16	1.08 ± 0.01
Xyloglucan + EDTA[d]	0.59 ± 0.05	-5.15 ± 0.06	-12.7 ± 1.68	-7.53 ± 1.64	1.04 ± 0.08
Galactose + calcium[b]	0.41 ± 0.003	-3.58 ± 0.01	-9.58 ± 0.12	-6.0 ± 0.18	1.02 ± 0.02
Galactose + EDTA[b]	0.38 ± 0.013	-3.32 ± 0.01	-9.40 ± 0.17	-6.08 ± 0.16	1.12 ± 0.11

[a] The ITC data were fitted to a single site binding model for all ligands. For polysaccharide ligands in which the molar concentration of binding sites is unknown, the *n* value was iteratively fitted to as close as possible to one, by adjusting the molar concentration of the ligand.
[b] *Ct*CBM62 was dialyzed in the presence of 2 mM CaCl$_2$, and the metal was added to the ITC experiment.
[c] *Ct*CBM62 was dialyzed in buffer lacking CaCl$_2$, and ITC was carried out in the absence of calcium.
[d] *Ct*CBMX was dialyzed into buffer lacking CaCl$_2$, and the ITC was performed in the presence of 10 mM EDTA.

binding to *XXX*G, suggests that the backbone components of mannan and xyloglucan do not make significant interactions with the protein. It should be noted, however, that the affinity of the protein for Gal and ^{1}6-α-GalMan$_3$ is 2 orders of magnitude lower than for galactomannan, whereas the K_a values for the xyloglucan oligosaccharides are also significantly lower than for the corresponding polysaccharide (Table 3). As mature *Ct*Xyl5A (which includes all the GH5-CBM6-CBM13-Fn3-CBM62-Doc1 domains) also exhibits much higher affinity for xyloglucan and carob galactomannan than galactose (Table 3), *Ct*CBM62 displays its polysaccharide targeting function in the full-length enzyme. To summarize, the capacity of *Ct*CBM62 to bind to xyloglucan and galactomannan is conferred by its recognition of either α- or β-D-galactose.

CtCBM62 Displays Avidity Effects—The tighter binding of *Ct*CBM62 to polysaccharides, compared with monovalent oligosaccharides and monosaccharides, is likely mediated through avidity effects, which occurs when a protein with multiple binding sites interacts with a multivalent ligand, such as a polysaccharide. Indeed, avidity effects are invariably associated with cross-linking and thus precipitation of the ligand-protein complex (18), which occurs when *Ct*CBM62 binds to xyloglucan, galactomannan, and arabinogalactan (data not shown).

To explore the potential role of calcium (which plays a key role in cellulosome function (40)) in the avidity effects displayed by *Ct*CBM62, the capacity of the protein to bind to xyloglucan and galactose was assessed in the presence of EDTA and calcium, respectively. The data, displayed in Table 4, show that for the simple monovalent ligand galactose, neither the addition of calcium nor the chelating agent EDTA influenced affinity for these carbohydrates. By contrast, *Ct*CBM62 binds to the galactose-containing polysaccharide xyloglucan >100-fold more tightly in the presence of calcium than with EDTA. The data described above indicate that calcium enhances affinity for multivalent ligands but does not influence the recognition of carbohydrates containing a single galactose residue. The most likely explanation for the role of calcium is through its capacity to mediate oligomerization of *Ct*CBM62, which would result in enhanced affinity for multivalent ligands through avidity effects. To explore this possibility, *Ct*CBM62 was subjected to
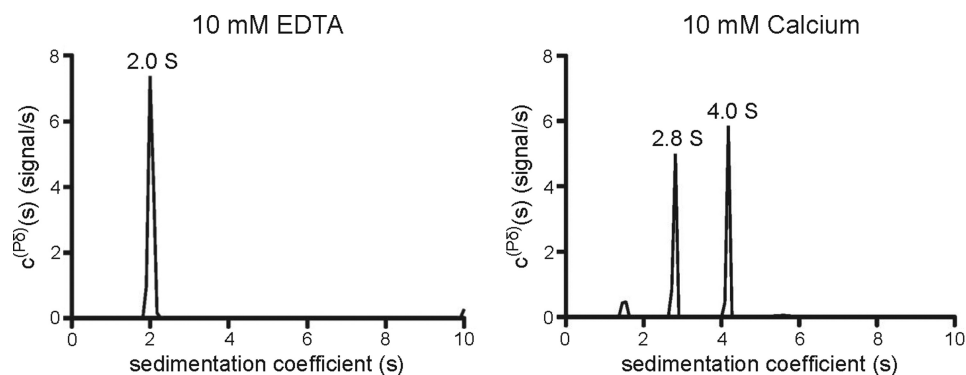
FIGURE 3. **Analytical ultracentrifugation of *Ct*CBM62.** Sedimentation velocity centrifugation was carried out as described under "Experimental Procedures." Freshly prepared protein was dialyzed against 4000 volumes of 20 mM Na-HEPES buffer, pH 7.0, containing 10 mM $CaCl_2$ or 10 mM EDTA. *Ct*CBM62 was centrifuged at a concentration of 1 mg/ml at 20 °C.
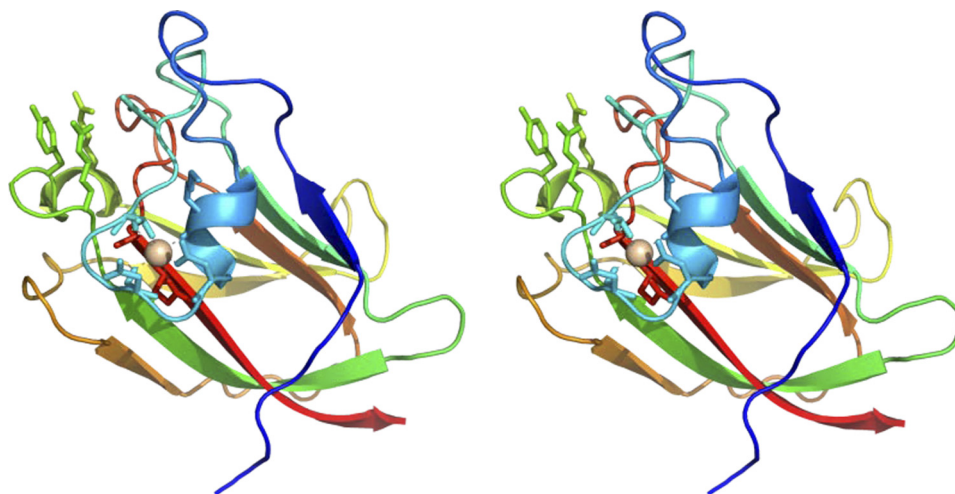

FIGURE 4. **Crystal structure of *Ct*CBM62 and the location residues that interact with galactose and calcium.** Stereo figure of the overall structure of *Ct*CBM62 displayed as a protein schematic, continuously color ramped from N to C terminus, from *blue* to *red*. The bound calcium is drawn as a *light pink sphere*, with coordinating amino acids drawn as *sticks*, with the H-bonds between them as *dashed lines*. The carbohydrate-binding amino acids are also drawn as *sticks*, and the same view is used for the other structural figures.

size exclusion chromatography, using a Sephadex S100 column. In the presence of EDTA, *Ct*CBM62 was eluted in a volume of 89 ml. Replacing the chelating agent with calcium reduced the elution volume to 74 ml (data not shown). Based on the calibration of the column with proteins of known molecular weights, *Ct*CBM62 migrated as a monomer in the presence of EDTA and a dimer when calcium was included in the elution buffer. Calcium-mediated oligomerization of *Ct*CBM62 was confirmed using analytical ultracentrifugation. In the presence of EDTA, *Ct*CBM62 sediments as a monomer with a sedimentation coefficient of 2.0 S. Calcium induces *Ct*CBM62 to form a dimer at 4.2 S that is in dynamic equilibrium with the monomer, causing a shift to 2.8 S (Fig. 3). These data indicate that the capacity of calcium to enhance the affinity of *Ct*CBM62 for multivalent ligands is mediated by metal ion-dependent oligomerization of the protein, which leads to avidity effects.

Crystal Structure of CtCBM62—To explore the mechanism by which *Ct*CBM62 binds to both α- or β-D-galactose, the crystal structure of the protein module was determined. In the conditions used to obtained crystals of the protein, no calcium was added, and thus the CBM crystallized in its monomeric form. The final structure corresponds to residues 739–878 of full-length *Ct*Xyl5A. *Ct*CBM62 displays a canonical β-sandwich fold (2) comprising two β-sheets containing five antiparallel β-strands on the concave face (β-strands 1, 2, 4, 5, and 7) and three antiparallel β-strands on the convex face (β-strands 3, 6, and 8) (Fig. 4). The protein contains a bound metal located at the beginning of the loop connecting α-1 helix to the β-2 strand which, based on its *B*-factor in comparison to neighboring atoms, its octahedral coordination, the bond distances, its satisfactory refinement with no residual positive or negative difference density, and its interaction with only oxygen ligands, has been modeled as calcium. This structural calcium is conserved in many CBM families that display a β-sandwich fold (2). *Ct*CBM62 displays greatest structural similarity to *Mv*CBM32 (PDB code 1EUT (41) r.m.s.d. of 2.7 Å over 131 Cα atoms), *Cp*CBM32 (PDB code 2J1A (42) r.m.s.d. of 2.4 Å over 126 Cα atoms), and *Sp*CBM47 (PDB code 2J1R (43) r.m.s.d. of 2.3 Å over 125 Cα atoms). These proteins all display <14% sequence identity with *Ct*CBM62.

Inspection of the surface of the protein reveals a shallow pocket formed by the loops connecting β-1 and α-1, α-1 and β-2, β-2 and α-2, although α-2 also contributes to the pocket (Fig. 5), a topology consistent with the specificity of the protein for the terminal sugars of complex polysaccharides. The crystal structure of *Ct*CBM62 in complex with [1]6-α-D-GalMan₃ or

*XLX*G confirms that the pocket includes the ligand-binding site and provides insight into how the protein recognizes the galactosyl residue, which makes identical interactions with the protein in both ligand complexes. Thus, the α-face of the pyranose ring of the bound galactose makes extensive hydrophobic contacts with Trp-754, which is aligned parallel to the sugar ring. Such hydrophobic interactions are a generic feature of CBM ligand recognition (12–14, 19, 44). The bound galactose also makes several direct hydrogen bonds with the protein; O1 and O2 make polar contacts with the OH of Tyr-806, whereas O3 forms hydrogen bonds with Nη1 and Nη2 of Arg-803 and Oδ2 of Asp-774. The O4 of galactose makes numerous potential polar interactions with *Ct*CBM62; the hydroxyl is within hydrogen bonding distance of Oδ1 and Oδ2 of Asp-774 and Nη1 of Arg-803 and Arg-809. Finally, the endocyclic oxygen of the galactose makes a polar contact with Nη2 of Arg-809. The extensive interactions made by *Ct*CBM62 with the axial O4 galactose explains why the protein displays tight specificity for this sugar; an equatorial O4, evident in glucose, mannose, and xylose, would not make polar contacts with the protein and, indeed, is predicted to make steric clashes with the side chain of Asp-774. Affinity gel electrophoresis (Fig. 6) and ITC (data not shown) showed that the replacement by alanine of all these residues resulted in the complete loss in ligand binding, confirming the role of these amino acids in galactose recognition. By contrast, mutation of residues on the concave surface of the protein, W782A, D786A, E789A, Q816A, E821A, F823A, and R856A (Fig. 6) did not appear to cause a reduction in affinity for xyloglucan. Similar observations were made with galactomannan and arabinogalactan (data not shown). These data confirm that the sugar-binding site in *Ct*CBM62 is located in the loops connecting the two β-sheets and not on the concave surface of the protein.

Significantly, *Ct*CBM62 does not make polar contact with the O6 of galactose suggesting that the protein may interact with L-arabinopyranose in which O4 is also axial. Data presented in Table 3 confirm that *Ct*CBM62 does bind to arabinopyranose, albeit with lower affinity than galactose. This may reflect the strain imposed by forcing the sugar ring into its pyranose conformation.

In both ligand complexes, components of the oligosaccharides, in addition to the terminal galactose, are evident. Indeed the successive Gal-β-Xyl and Xyl-α-Glc linkages in *XLX*G curve the xyloglucan oligosaccharide into a shape that is perfectly accommodated by the surface of *Ct*CBM62. These topological features may contribute to the slightly higher affinity of the protein for *XLX*G, compared with galactose; the increase in affinity may reflect polar interactions between the Glc backbone and residues (Gly-805 and Gly-862; Fig. 5) on the surface of the protein. To accommodate the Glc or Man backbone of *XLX*G and ^{1}6-α-D-GalMan$_3$, respectively, the side chain of Gln-809 is twisted by 114º which, although imposing an energetic cost, enables both Oϵ1 and Nϵ2 of this residue to make polar contacts with the backbone of at least xyloglucan. By contrast, the Man backbone of ^{1}6-α-D-GalMan$_3$ did not make direct polar interactions with *Ct*CBM62.

As discussed above, *Ct*CBM62 appears to undergo calcium-mediated oligomerization leading to increased affinity for polysaccharides through avidity effects. Inspection of the structure of *Ct*CBM62 reveals a calcium-binding site that is conserved in several other CBM families that display a jelly roll fold (CBM4, CBM6, CBM22, and CBM29 (2)). The calcium ion makes coordinate bonds with the O of Lys-763, Oδ1 of Asp-766, O of Asp-766, the backbone O, and Oγ of Thr-771, O of Ala-868, and Oϵ1 of Glu-869, Fig. 4, and as such it fulfills the octahedral geometry typical of many calcium-binding sites. The calcium-binding loop contributes to a crystal packing interface with a symmetry-equivalent molecule in an adjacent asymmetric unit. The physicochemical characteristics of this particular interface are not greatly dissimilar from other potential dyad interactions in the crystal. The D766A, T771A, E869A, D766A/E869A and D766A/T771A/E869A mutants of *Ct*CBM62 (in which the calcium-binding site has been disrupted by mutating, in various combinations, the three residues whose side chains make polar contacts with the metal) displayed calcium-dependent high affinity for xyloglucan, supplemental Table S2. Thus, the calcium-binding loop does not appear to contribute to the oligomerization of the protein in solution. Attempts to map the dimer-binding site by replacing all the surface Asp and Glu residues with alanine (mutations listed in supplemental Table S2) failed to influence the avidity effects displayed by the protein. Thus, currently, the site of *Ct*CBM62 oligomerization remains unclear.

*Ct*CBM62 Defines a New CBM Family—*Ct*CBM62 was subjected to BLAST analysis to identify other proteins that are related to the CBM. The analysis revealed that *Ct*CBM62 displayed very distant similarity to a CBM32 module, comprising residues 2086–2229 in the *Caldicellulosiruptor kronotskyensis* protein Calkro_0121 (BLAST score of $7e^{-4}$), with significant sequence identity restricted to the N-terminal 17 residues of the two protein modules. No sequence similarity was identified between *Ct*CBM62 and any other CAZy protein, including the remaining 1000 CBM32 modules. Thus. *Ct*CBM62 represents the founding member of a new CBM family, defined as CBM62. The BLAST search, however, identified five non-CAZy protein modules that display >42% sequence identity with *Ct*CBM62 with *e* values $<10^{-23}$ (supplemental Fig. S2). These proteins are therefore likely to be members of family CBM62. Two of these CBM62 modules are components of large extracytoplasmic proteins of unknown function, although the other three contain members of glycoside hydrolase families. The residues that comprise the ligand-binding site in *Ct*CBM62 are highly conserved in the five proteins suggesting that they may also bind to galactose (and arabinopyranose). Indeed, one of these proteins, C7IBP5, is a member of family GH98, where endo-β-galactosidase is the only reported activity. In addition to the five close homologs, there are 40 proteins that also show sequence similarity with *Ct*CBM62 with *e* values $<10^{-5}$. The limited sequence similarity is generally restricted to the C-terminal portion of *Ct*CBM62. Closer analysis, however, showed that noncontiguous regions of *Ct*CBM62 display extensive sequence similarity with these proteins. When a rearranged linear sequence of one of these proteins, a conserved hypothetical protein from *Parbacteroides distasonis* (GenBank^{TM} accession number ABR45148), in which the N- and C-terminal regions are permuted at position 69 (the N-terminal Phe-466 and
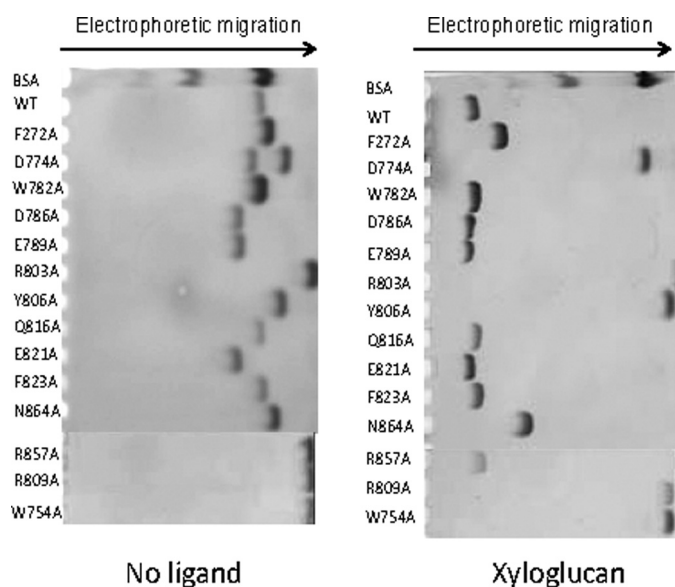
CBM62/XLXG
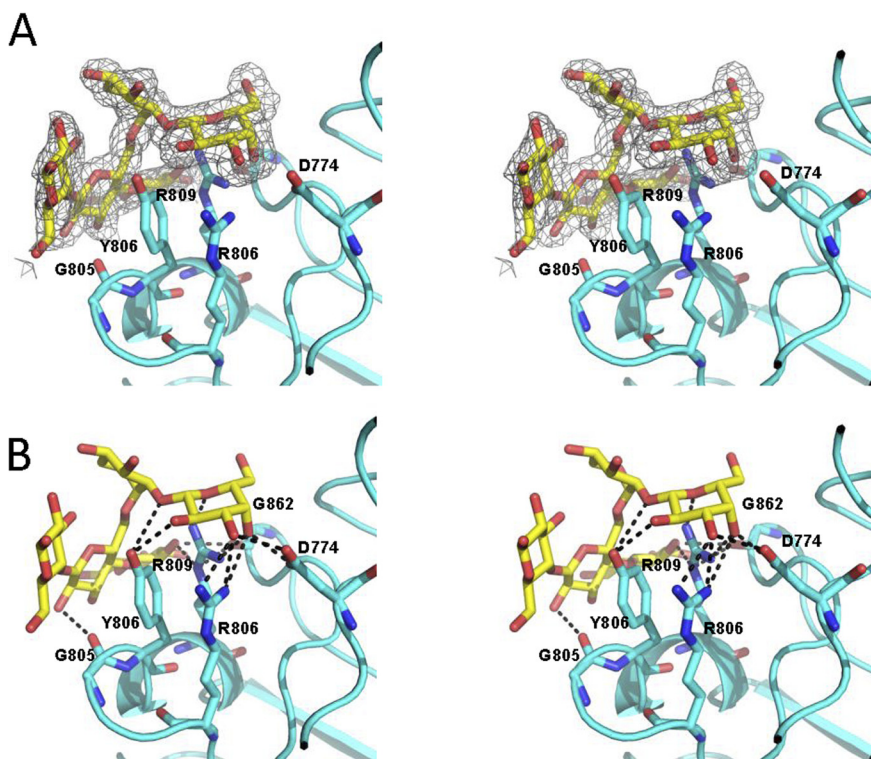
*Ct*CBM62/^{1}6-α- D-GalMan$_3$
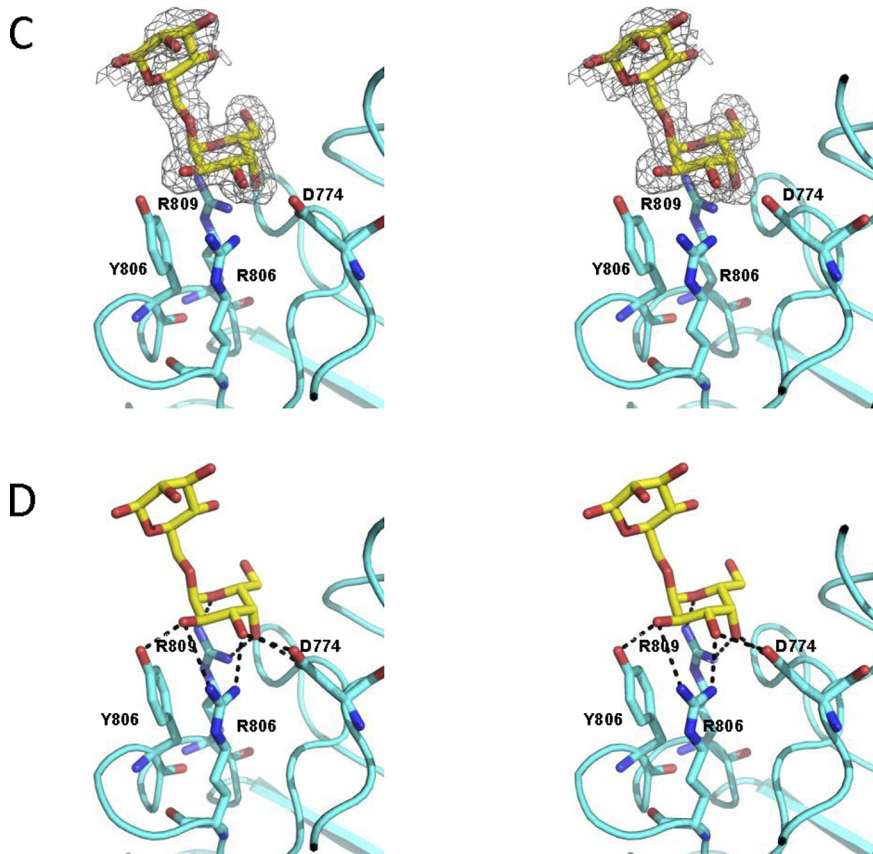
FIGURE 6. **Affinity gel electrophoresis of wide type and mutants of CtCBM62 against xyloglucan.** Wide type and mutants of *Ct*CBM62 were electrophoresed on nondenaturing polyacrylamide gels containing no ligand or 1 mg/ml xyloglucan. BSA was used as a nonpolysaccharide binding control.

C-terminal Asn-600 residues are ligated together and cleavage of the protein occurs between Asn-535 and Asp-536), is compared with *Ct*CBM62, then sequence similarity with the apparent "noncontiguous homologs" extends across the whole sequence of the CBM. Thus, the proteins display noncontiguous stretches of homology with a score of $3e^{-7}$. If *Ct*CBM62 is compared with the rearranged *Parbacteroides* protein, then sequence similarity is contiguous with an amino acid identity of ~40% and a score of e^{-17} (Fig. 7 and supplemental Fig. S2). The sequence similarity of noncontiguous regions of these proteins is strongly indicative of a "circular permutation." In this process, genetic events result in the ligation of the terminal residues of the protein, which is subsequently cleaved to yield a new N and C terminus (45, 46). The cleavage or ligation event likely occurred in CBM62 members at a position equivalent to the peptide bond linking Gly-797 and Tyr-798 in *Ct*CBM62.

The vast majority of CBM families display a β-sandwich fold in which the strand order and a structural calcium are highly conserved features (2). It is therefore likely that these families arose from a common progenitor sequence. As the β-strand order in *Ct*CBM62 is similar to other CBM families (*e.g.* CBM4, -6, -15, -22, -29, -35, and -36), it is unlikely that the protein module arose through a circular permutation event. It would therefore appear that a cleavage and ligation event occurred in an ancestral member of CBM62, which resulted in the large number of proteins that display noncontiguous sequence similarity to *Ct*CBM62. It should be noted that alignment of these noncontiguous sequences with (rearranged) *Ct*CBM62 shows that the key ligand-binding residues are highly conserved, sug-

gesting that these proteins may also target terminal galactose residues. In general, proteins that have been subjected to circular permutation adopt a β-barrel or β-sandwich fold in which the N and C termini are in close proximity. Circular permutation events have been observed in a range of enzymes, including those that modify carbohydrates (45, 46). As CBMs generally display a β-sandwich fold in which the two termini are in close proximity (2), these proteins are candidates for permutation events. Indeed, a recent report has shown that CBM36 and CBM60 display highly conserved ligand-binding sites derived from different regions of the respective proteins, which likely reflect a circular permutation event (22). The evolutionary rationale (if any) for circular permutation events is not entirely clear. Intuitively, such events, which retain overall three-dimensional structure, may introduce subtle structural changes that alter the function of the protein. In view of the circular permutation event within CBM62, we suggest the division of the family into two subfamilies. The two subfamilies display contiguous sequence similarity to *Ct*CBM62 or are related to the protein by a circular permutation event, respectively.

DISCUSSION

This study reveals a novel CBM family that recognizes galactose-containing polysaccharides, which is located in an enzyme that displays arabinoxylanase activity (the catalytic module is described in the accompanying paper (38)), and is a component of the *C. thermocellum* cellulosome. The β-sandwich fold displayed by *Ct*CBM62 is typical of the majority of CBM families (2). Although historically the ligand-binding site of CBMs is associated with the concave surface of these proteins, this appears to apply only to proteins that recognize the internal regions of polysaccharides. The location of the *Ct*CBM62 ligand-binding site in the loops that connect the β-sheets is an example of an increasingly common feature of CBMs that recognize terminal sugars (8, 16, 22, 47).

An intriguing feature of *Ct*Xyl5A is that the enzyme contains a CBM that binds terminal D-galactose or L-arabinopyranose residues of polysaccharides, a specificity mediated by numerous interactions with the axial O4, which distinguishes these two sugars from other neutral carbohydrates, notably mannose, xylose, and glucose, which are widely distributed in plant structural polysaccharides (48). In general, plant cell wall hydrolases contain CBMs that target the substrate recognized by the enzyme and/or crystalline cellulose (2). Although most arabinoxylans contain arabinofuranose and 4-O-methyl-D-glucuronic acid side chains, it is apparent that these polysaccharides are very heterogeneous molecules, and eucalyptus contains arabinoxylans that are also decorated with D-galactose (49). It is therefore possible that the primary substrate for *Ct*Xyl5A is an arabinoxylan that also contains sugar side chains (D-galactose) recognized by *Ct*CBM62. Such a targeting strategy has resonance with the observation that a CBM32 targets LacNAc

FIGURE 5. **Structure of CtCBM62 in complex with xyloglucan and galactomannan-derived oligosaccharides.** *A* and *C* display the stereo figure of the carbohydrate-binding site of *Ct*CBM62, with unbiased F_o-F_c electron density displayed as a mesh and key amino acids and the carbohydrates drawn as *sticks*. The protein backbone is shown for reference. In the *XLXG* complex, the electron density is contoured at 3σ, 0.14 e$^-$/Å^3, and for GM3, the map is also at 3σ, e$^-$/Å^3. *B* and *D* display the same view as *A* and *C*, respectively, of the carbohydrate-binding site of *Ct*CBM62, with hydrogen bonds drawn as *dashed lines* and key amino acids labeled. In both *B* and *D* only the amino acids that make hydrogen bonds with the ligand are shown.
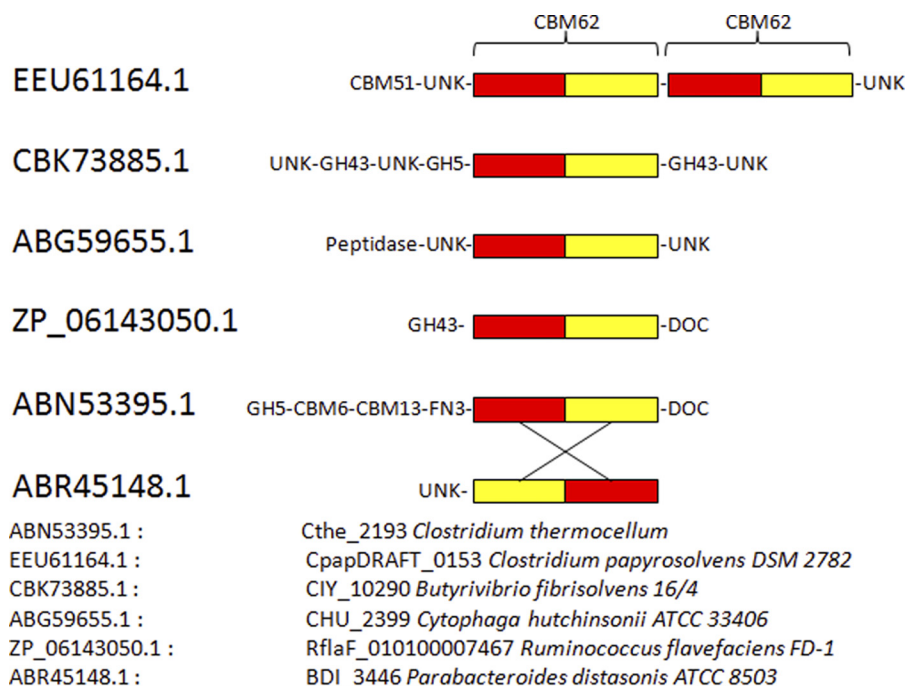
FIGURE 7. **Circular permutation in the CBM62 family.** BLAST analysis of *Ct*CBM62, corresponding to residues 739–885 of *Ct*Xyl5A, identified five proteins that displayed >42% sequence identity, which are identified by their GenBank™ accession numbers. ABR45148.1 is an example of a group of 40 proteins that display noncontiguous similarity to *Ct*CBM62. Extensive co-linear identity to *Ct*CBM62 is evident after ABR45148.1 has been subject to a circular permutation. This genetic event is indicated by the crossover lines, leading to the ligation of the N and C terminus of the encoded protein and cleavage at the interface of the *red* and *yellow* sequence, resulting in the generation of a new N and C terminus. The sequence alignment of *Ct*CBM62 (ABN53395) and ABR45148 before and after circular permutation is shown in supplemental Fig. S2.

(Gal-β1,4-GlcNAc), but the appended enzymes functions as an *N*-acetyl-β-hexosaminidase (42). Recent studies, however, have shown that CBMs may direct their appended enzymes to their target substrates by binding to a polysaccharide that is in close proximity with the substrate. Examples include xylanases and pectinases appended to cellulose-specific CBMs (50). It is therefore possible that arabinoxylans are in close association with xyloglucans, galactomannans, and/or arabinogalactans in certain cell walls, and by targeting the β- and α-D-galactose or L-arabinopyranose residues, *Ct*CBM62 brings the catalytic module of *Ct*Xyl5A into close proximity with its substrate.

The observations that *Ct*CBM62 binds more tightly to complex polysaccharides than to monovalent ligands and binding is associated with the formation of an insoluble polysaccharide lattice are classic features of avidity effects (18, 20). The rationale for the increase in K_a relates to the decrease in the frequency with which the protein will completely dissociate from its complex ligand, compared with monovalent carbohydrates. Examples of such avidity effects have been observed previously in enzymes containing multiple CBMs that recognize the same complex ligand (17, 18). By contrast, avidity effects through the oligomerization of a discrete enzyme-located CBM, as observed here for *Ct*CBM62, have not been reported previously, although such events are a very common feature of plant and animal lectins (20).

Analysis of the structure of derivatives of *Ct*Xyl5A showed that only *Ct*CBM62 was capable of dimerization (data not shown). The biological significance of calcium-induced dimerization of *Ct*CBM62, within the context of full-length *Ct*Xyl5A, is particularly intriguing when one considers that the module is derived from a protein that is a component of the cellulosome. The cellulosome assembles through the interaction of the dockerin module, present on the enzymes, with one of the nine cohesins located on the noncatalytic scaffoldin protein, CipA (for review see Refs. 21, 40). It is possible that calcium-induced dimerization of *Ct*CBM62 recruits two molecules of *Ct*Xyl5A onto the same cellulosome molecule. The oligomerization, however, may also lead to cellulosome cross-linking (if the dockerins in the dimer bind to different molecules of CipA), and thus contribute to the formation of polycellulosomes, which are formed on the surface of the bacterium (11).

In conclusion, this report reveals a novel CBM that represents the founding member of family 62. *Ct*CBM62 binds to the terminal D-galactose and L-arabinopyranose residues in polysaccharides, specificities not previously observed in CBMs that are components of the *C. thermocellum* cellulosome. The CBM uniquely mediates protein dimerization, which confers polysaccharide, rather than oligosaccharide, targeting through avidity effects. The catalytic module appended to *Ct*CBM62 is an arabinoxylanase (described in the accompanying paper (38)), suggesting that the enzyme targets xylans that contain a highly complex repertoire of side chains.

REFERENCES

1. Ragauskas, A. J., Williams, C. K., Davison, B. H., Britovsek, G., Cairney, J., Eckert, C. A., Frederick, W. J., Jr., Hallett, J. P., Leak, D. J., Liotta, C. L., Mielenz, J. R., Murphy, R., Templer, R., and Tschaplinski, T. (2006) *Science* **311,** 484–489
2. Boraston, A. B., Bolam, D. N., Gilbert, H. J., and Davies, G. J. (2004) *Biochem. J.* **382,** 769–781
3. Black, G. W., Rixon, J. E., Clarke, J. H., Hazlewood, G. P., Ferreira, L. M.,

Bolam, D. N., and Gilbert, H. J. (1997) *J. Biotechnol.* **57,** 59–69

4. Bolam, D. N., Ciruela, A., McQueen-Mason, S., Simpson, P., Williamson, M. P., Rixon, J. E., Boraston, A., Hazlewood, G. P., and Gilbert, H. J. (1998) *Biochem. J.* **331,** 775–781

5. Ferreira, L. M., Durrant, A. J., Hall, J., Hazlewood, G. P., and Gilbert, H. J. (1990) *Biochem. J.* **269,** 261–264

6. Cantarel, B. L., Coutinho, P. M., Rancurel, C., Bernard, T., Lombard, V., and Henrissat, B. (2009) *Nucleic Acids Res.* **37,** D233–D238

7. Czjzek, M., Bolam, D. N., Mosbah, A., Allouch, J., Fontes, C. M., Ferreira, L. M., Bornet, O., Zamboni, V., Darbon, H., Smith, N. L., Black, G. W., Henrissat, B., and Gilbert, H. J. (2001) *J. Biol. Chem.* **276,** 48580–48587

8. Henshaw, J., Horne-Bitschy, A., van Bueren, A. L., Money, V. A., Bolam, D. N., Czjzek, M., Ekborg, N. A., Weiner, R. M., Hutcheson, S. W., Davies, G. J., Boraston, A. B., and Gilbert, H. J. (2006) *J. Biol. Chem.* **281,** 17099–17107

9. Henshaw, J. L., Bolam, D. N., Pires, V. M., Czjzek, M., Henrissat, B., Ferreira, L. M., Fontes, C. M., and Gilbert, H. J. (2004) *J. Biol. Chem.* **279,** 21552–21559

10. van Bueren, A. L., Morland, C., Gilbert, H. J., and Boraston, A. B. (2005) *J. Biol. Chem.* **280,** 530–537

11. Mayer, F., Coughlan, M. P., Mori, Y., and Ljungdahl, L. G. (1987) *Appl. Environ. Microbiol.* **53,** 2785–2792

12. Raghothama, S., Simpson, P. J., Szabó, L., Nagy, T., Gilbert, H. J., and Williamson, M. P. (2000) *Biochemistry* **39,** 978–984

13. Simpson, P. J., Xie, H., Bolam, D. N., Gilbert, H. J., and Williamson, M. P. (2000) *J. Biol. Chem.* **275,** 41137–41142

14. Pell, G., Williamson, M. P., Walters, C., Du, H., Gilbert, H. J., and Bolam, D. N. (2003) *Biochemistry* **42,** 9316–9323

15. Jamal-Talabani, S., Boraston, A. B., Turkenburg, J. P., Tarbouriech, N., Ducros, V. M., and Davies, G. J. (2004) *Structure* **12,** 1177–1187

16. Montanier, C., van Bueren, A. L., Dumon, C., Flint, J. E., Correia, M. A., Prates, J. A., Firbank, S. J., Lewis, R. J., Grondin, G. G., Ghinet, M. G., Gloster, T. M., Herve, C., Knox, J. P., Talbot, B. G., Turkenburg, J. P., Kerovuo, J., Brzezinski, R., Fontes, C. M., Davies, G. J., Boraston, A. B., and Gilbert, H. J. (2009) *Proc. Natl. Acad. Sci. U.S.A.* **106,** 3065–3070

17. Bolam, D. N., Xie, H., White, P., Simpson, P. J., Hancock, S. M., Williamson, M. P., and Gilbert, H. J. (2001) *Biochemistry* **40,** 2468–2477

18. Boraston, A. B., McLean, B. W., Chen, G., Li, A., Warren, R. A., and Kilburn, D. G. (2002) *Mol. Microbiol.* **43,** 187–194

19. Charnock, S. J., Bolam, D. N., Nurizzo, D., Szabó, L., McKie, V. A., Gilbert, H. J., and Davies, G. J. (2002) *Proc. Natl. Acad. Sci. U.S.A.* **99,** 14077–14082

20. Vijayan, M., and Chandra, N. (1999) *Curr. Opin. Struct. Biol.* **9,** 707–714

21. Bayer, E. A., Belaich, J. P., Shoham, Y., and Lamed, R. (2004) *Annu. Rev. Microbiol.* **58,** 521–554

22. Correia, M. A., Abbott, D. W., Gloster, T. M., Fernandes, V. O., Prates, J. A., Montanier, C., Dumon, C., Williamson, M. P., Tunnicliffe, R. B., Liu, Z., Flint, J. E., Davies, G. J., Henrissat, B., Coutinho, P. M., Fontes, C. M., and Gilbert, H. J. (2010) *Biochemistry* **49,** 6193–6205

23. Tormo, J., Lamed, R., Chirino, A. J., Morag, E., Bayer, E. A., Shoham, Y., and Steitz, T. A. (1996) *EMBO J.* **15,** 5739–5751

24. Carvalho, A. L., Goyal, A., Prates, J. A., Bolam, D. N., Gilbert, H. J., Pires, V. M., Ferreira, L. M., Planas, A., Romão, M. J., and Fontes, C. M. (2004) *J. Biol. Chem.* **279,** 34785–34793

25. Charnock, S. J., Bolam, D. N., Turkenburg, J. P., Gilbert, H. J., Ferreira, L. M., Davies, G. J., and Fontes, C. M. (2000) *Biochemistry* **39,** 5013–5021

26. Dvortsov, I. A., Lunina, N. A., Chekanovskaya, L. A., Schwarz, W. H., Zverlov, V. V., and Velikodvorskaya, G. A. (2009) *Microbiology* **155,** 2442–2449

27. Najmudin, S., Guerreiro, C. I., Carvalho, A. L., Prates, J. A., Correia, M. A., Alves, V. D., Ferreira, L. M., Romão, M. J., Gilbert, H. J., Bolam, D. N., and Fontes, C. M. (2006) *J. Biol. Chem.* **281,** 8815–8828

28. Freelove, A. C., Bolam, D. N., White, P., Hazlewood, G. P., and Gilbert, H. J. (2001) *J. Biol. Chem.* **276,** 43010–43017

29. Brown, P. H., and Schuck, P. (2006) *Biophys. J.* **90,** 4651–4661

30. Brown, P. H., Balbo, A., and Schuck, P. (2007) *Biomacromolecules* **8,** 2011–2024

31. Kabsch, W. (2010) *Acta Crystallogr.* **D66,** 125–132

32. Evans, P. (1993) *CCP4 Daresbury Study Weekend: Data Collection and Processing, DL/SCI/R34*, pp. 114–122, Daresbury Laboratory, Warrington, UK

33. Schneider, T. R., and Sheldrick, G. M. (2002) *Acta Crystallogr. D Biol. Crystallogr.* **58,** 1772–1779

34. Sheldrick, G. M. (1990) *Acta Crystallogr. A* **46,** 467–473

35. Emsley, P., and Cowtan, K. (2004) *Acta Crystallogr. D Biol. Crystallogr.* **60,** 2126–2132

36. Collaborative Computational Project No. 4 (1994) *Acta Crystallogr. D Biol. Crystallogr.* **50,** 760–763

37. Murshudov, G. N., Vagin, A. A., and Dodson, E. J. (1997) *Acta Crystallogr. D Biol. Crystallogr.* **53,** 240–255

38. Correia, A. S., Mazumder, K., Bras, J. L., Firbank, S. J., Zhu, Y., Lewis, R. J., York, W. S., Fontes, C. M., and Gilbert, H. J. (2011) *J. Biol. Chem.* **286,** ********

39. Gloster, T. M., Ibatullin, F. M., Macauley, K., Eklöf, J. M., Roberts, S., Turkenburg, J. P., Bjørnvad, M. E., Jørgensen, P. L., Danielsen, S., Johansen, K. S., Borchert, T. V., Wilson, K. S., Brumer, H., and Davies, G. J. (2007) *J. Biol. Chem.* **282,** 19177–19189

40. Fontes, C. M., and Gilbert, H. J. (2010) *Annu. Rev. Biochem.* **79,** 655–681

41. Gaskell, A., Crennell, S., and Taylor, G. (1995) *Structure* **3,** 1197–1205

42. Ficko-Blean, E., and Boraston, A. B. (2006) *J. Biol. Chem.* **281,** 37748–37757

43. Boraston, A. B., Wang, D., and Burke, R. D. (2006) *J. Biol. Chem.* **281,** 35263–35271

44. Nagy, T., Simpson, P., Williamson, M. P., Hazlewood, G. P., Gilbert, H. J., and Orosz, L. (1998) *FEBS Lett.* **429,** 312–316

45. Lindqvist, Y., and Schneider, G. (1997) *Curr. Opin. Struct. Biol.* **7,** 422–427

46. Lo, W. C., Lee, C. C., Lee, C. Y., and Lyu, P. C. (2009) *Nucleic Acids Res.* **37,** D328–D332

47. Abbott, D. W., Ficko-Blean, E., van Bueren, A. L., Rogowski, A., Cartmell, A., Coutinho, P. M., Henrissat, B., Gilbert, H. J., and Boraston, A. B. (2009) *Biochemistry* **48,** 10395–10404

48. Brett, C. T., and Waldren, K. (1996) *Physiology and Biochemistry of Plant Cell Walls. Topics in Plant Functional Biology*, Chapman and Hall Ltd., London

49. Shatalov, A. A., Evtuguin, D. V., and Pascoal Neto, C. (1999) *Carbohydr. Res.* **320,** 93–99

50. Hervé, C., Rogowski, A., Blake, A. W., Marcus, S. E., Gilbert, H. J., and Knox, J. P. (2010) *Proc. Natl. Acad. Sci. U.S.A.* **107,** 15293–15298
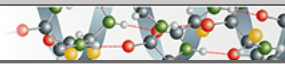
Cedric Y. Montanier, Márcia A. S. Correia,
James E. Flint, Yanping Zhu, Arnaud Baslé,
Lauren S. McKee, José A. M. Prates, Samuel
J. Polizzi, Pedro M. Coutinho, Richard J.
Lewis, Bernard Henrissat, Carlos M. G. A.
Fontes and Harry J. Gilbert

Access the most updated version of this article at doi: 10.1074/jbc.M110.217372

Find articles, minireviews, Reflections and Classics on similar topics on the JBC Affinity Sites.

Alerts:

- When this article is cited
- When a correction for this article is posted

Click here to choose from all of JBC's e-mail alerts

Supplemental material:

http://www.jbc.org/content/suppl/2011/03/29/M110.217372.DC1.html

This article cites 47 references, 21 of which can be accessed free at
http://www.jbc.org/content/286/25/22499.full.html#ref-list-1